Original Paper Environ. Control Biol., **44** (4), 245–255, 2006

Non-Destructive Estimation of Firmness of Strawberries (*Fragaria*×*ananassa Duch.*) Using NIR Hyperspectral Imaging

Jasper G. TALLADA, Masateru NAGATA* and Taichi KOBAYASHI

The United Graduate School of Agricultural Sciences, Kagoshima University, 1–21–24 Korimoto, Kagoshima 890–0065, Japan
** Faculty of Agriculture, University of Miyazaki, 1–1 Gakuen Kibanadai Nishi, Miyazaki 889–2192, Japan*

(Received May 17, 2006)

The non-destructive estimation of internal quality of fruits for on-line grading to achieve higher product consistency and enhanced safety will greatly benefit the consumer and the fruit industry as a whole. This research was aimed at developing prediction models for firmness in strawberries (*Fragaria*×*ananassa Duch.*) using NIR hyperspectral imaging. From freshly harvested strawberries of "*Akihime*" variety at three levels of ripeness maturity, NIR (near infrared) hyperspectral images (650 to 1000 nm at 5 nm intervals) were taken and calibration models were developed using stepwise multiple linear regression. The three-wavelength (685, 865, and 985 nm) prediction model for firmness had a correlation and standard error for prediction of 0.786 and 0.350 MPa, respectively (50% to full-ripe group). The importance of chlorophyll absorbance peak at around 680 nm and peak of water at 980 nm was also confirmed.

Keywords : firmness, hyperspectral imaging, near infrared light, strawberry

INTRODUCTION

Consumers, while seeking for much better quality agricultural products, are becoming more concerned with consistency of items within a batch, and enhanced food safety. Common machine vision techniques had been successfully employed to monitor external product quality such as size, shape and color (Chen et al., 2002). However, greater attention is now focused on non-destructive estimation of internal quality and detection of external defects and contamination (Kim et al., 2002).

In many fruits, firmness is a fine indicator of level of ripeness maturity and freshness, and hence, eating quality experience (Shewfelt and Prussia, 1993). It also indicates susceptibility of the fruits to physical damage when mechanically processed and transported to the market. With the recent interests on robotic harvesting of strawberries, ascertaining the level of firmness of fruits would dictate the level of force that the harvest hand should maximally apply for effective detachment and conveyance. To date, accurate measurement of firmness would require destructive approaches such as puncture and compression tests. There had been some non-destructive techniques being developed such as vibration and acoustic methods (De Ketelaere and De Baerdemaeker, 2001). Quite recently, optical approaches are being employed for fast and accurate on-line meas-

Corresponding author : Masateru Nagata, fax : +81–985–58–7246,
e-mail : nagatam@cc.miyazaki-u.ac.jp

urements.

Near infrared (NIR) spectroscopy had been proven useful for measuring some internal quality attributes such as total soluble solids, titratable acidity, dry matter, and starch content in the fruits kiwi, apple, strawberry and mango (McGlone and Kawano, 1998; Schaare et al., 2000; Lammertyn et al., 1998; Ito, 2002; Saranwong et al., 2004). The main shortcoming of this technique, however, is that measurements are confined only to a single patch or area on the fruit surface (Kim et al., 2001; Lu, 2003). Additionally, NIR spectroscopy requires consistency of measurement location since most fruits have spatially varying quality attributes (Peiris et al., 1999; Lu and Ariana, 2002). Spectral imaging offers an improved solution over NIR spectroscopy by analyzing images of the entire fruit in a narrow band of wavelength of light. While in hyperspectral imaging, many images are taken contiguously at a range of wavelengths having narrow intervals, a multi-spectral imaging system captures several images at a specific set of wavelengths (Abbott, 1999). Several researchers reckoned that the multi-spectral imaging technology would more likely be adapted in on-line grading systems because it is cost-effective and technically more feasible in high-speed operations (Kim et al., 2001; Abbott, 1999). But, it would require identification of specific center-wavelengths that could be determined through a hyperspectral imaging study.

Strawberry (*Fragaria×ananassa Duch.*) is a popular fruit in Japan that is often eaten fresh. There had been limited research in the use of spectral optical techniques in evaluation of quality in strawberries. Ito (2002) developed prediction models for sugar content in Brix in strawberries in the NIR range of 750 to 1100 nm. Using multiple linear regression analysis, he found the best predictors at 907 and 882 nm. Recently, spectral imaging is being employed to assess the internal qualities and detect bruising on strawberries. In 2001, Nagata et al. demonstrated an optical technique to judge bruising on strawberries using NIR imaging. While in 2004, Nagata et al. had shown the usefulness of estimating firmness and soluble solids content using hyperspectral imaging in the visible range (450 to 650 nm). In a recent work, Nagata et al. (2006) had used NIR hyperspectral imaging for the detection of bruises on strawberries at two levels of ripeness maturity.

The main goal of the research was to develop non-destructive techniques for estimation of internal quality of fruits for sorting and grading applications. Specifically, the research endeavored to formulate prediction models for firmness of strawberries using hyperspectral imaging in the near infrared range (650 to 1000 nm), and to identify specific set of wavelengths that can estimate firmness for a multi-spectral imaging system.

MATERIALS AND METHODS

1. Hyperspectral imaging set-up and procedure

The hyperspectral imaging system had a high-resolution charge-coupled device (CCD) camera, lens optics, a liquid crystal tunable filter, a tungsten-halogen light source and a cooler as shown in Fig. 1. The camera was a 14-bit Apogee AP2E (Apogee Instruments, Inc., Auburn, CA, USA) monochrome camera fitted with a Nikkor f/1.2 optical lens. A Varispec liquid crystal tunable filter (LCTF, Cambridge Research and Instrumentation, Massachusetts, USA) VS-NIR-20-10 (650 to 1100 nm, 10 nm full width at half maximum bandwidth) was attached to the lens. The Fiber-Lite PL950 DC regulated light source (Dolan-Jenner Industries, St. Lawrence, MA, USA) had a 150-watt 21V EKE tungsten-halogen quartz light bulb with the infrared cut-off filter removed. The fiber optic light guide was placed vertically above the platform. A cooler stabilized the temperature within the set-up to around 23°C.

A custom-built Visual Basic software controlled the MaxIm/DL (a software provided by the manufacturer to control the camera) and National Instruments LabView Cris3 (a software provided by the manufacturer to control the Varispec filter) programs. Spectral images of a set of fruits were

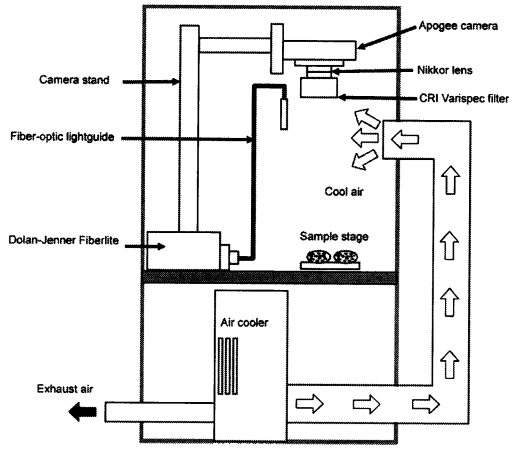

Fig. 1 Pictorial diagram of the hyperspectral imaging setup.

automatically acquired from 650 to 1000 nm at 5 nm intervals (71 images). The exposure time was varied from 0.70 to 7.25 s to account for the variable sensitivity of the system due to variable responsivity of the CCD sensor, transmission efficiency of the LCTF and spectral distribution of the light across the wavelength range as was earlier done by Evans et al. (1998) and Cogdill et al. (2004). Using the same settings, reference images from a 125×125 mm Spectralon reference panel (99% diffuse reflectance, SRT-99-050, Labsphere, Inc., North Sutton, NH, USA), and also with the camera shutter closed, dark current images were acquired at the start, for every 10 sets and at the end of image acquisition.

2. Experimental procedure

From a nearby greenhouse farm, about 210 pieces of strawberries of "*Akihime*" variety at three ripeness maturity levels (50–60% ripe, 70–80% ripe and full-ripe maturity based on extent of coverage of red color on fruit peel) were obtained. They were immediately brought to the laboratory for dimensional size (length, width and breadth) and mass measurements.

Six samples (two pieces from each ripeness maturity level) were randomly selected and randomly placed on a six-cell sample holder. Color images were acquired using a color CCD camera for documentation purposes and the samples were brought for hyperspectral imaging.

The samples were immediately subjected to firmness measurement right after the acquisition of spectral images. The instrument used was an Orientec Universal Testing Machine (UTM, STA-1150; Orientec Corporation, Japan) with a 3 mm diameter steel tip to an 8 mm penetration depth driven at a speed of 1.67 mm s^{-1} as shown in Fig. 2. The peak value for the measured stress was recorded in MPa.

3. Data processing and analysis

The images were processed using MATLAB version 6.5.1 and its Image Processing Toolbox (The Mathworks, Inc., Natick, MA, USA). Flat field correction was applied to compute the relative reflectance using the following equation:

$$I_{norm}(x,y) = \frac{I_{sample}(x,y) - I_{dark}(x,y)}{I_{reference}(x,y) - I_{dark}(x,y)} \cdot m \qquad (1)$$

where, $I_{norm}(x,y)$ is the normalized pixel value (relative reflectance) at pixel location (x,y); $I_{sample}(x,y)$, $I_{reference}(x,y)$, and $I_{dark}(x,y)$ are the pixel values for the sample, reference and dark images, respectively, at the same location (x,y); and m is a factor with a value of 1.0 based on the Spectralon reference panel.

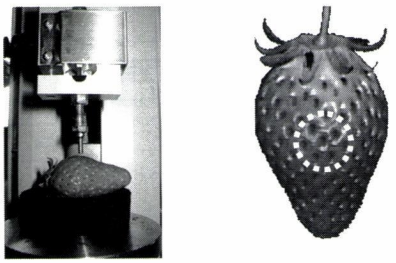

(a) (b)

Fig. 2 (a) Firmness measurements were taken using a 3 mm diameter steel probe tip from a central point in-between fruit achenes; (b) relative reflectance spectral data were obtained from the same area using a circular mask.

From the corrected images, the mean value of reflectance was computed from a spot (mask shown in Fig. 2(b)) about the same location where firmness measurements were taken on the fruit surface. The mean values were used for the firmness prediction model development.

A stepwise multiple linear regression analysis was carried out to determine the optimum set of wavelength values and to develop calibration models using the statistical software SPSS version 11 (Statistical Product and Service Solutions, SPSS Inc., USA). Many approaches for data analysis based on techniques of spectroscopic analysis (logarithmic transform, smoothing, zero-centering, differentiation, second-derivative, principal components, partial least squares and others) were reportedly used by previous researches (Schaare and Fraser, 2000; Martinsen and Schaare, 1998; Schmilovitch et al., 2000). In this work, the relative reflectance values from each wavelength were treated independently because a suitable set of wavebands for model development was being sought, and to keep the analysis as simple and yet useful as possible. Two groups of samples were considered, one group included only the 70–80% ripe and full-ripe samples, and the second group comprised the entire sample set (50–60% ripe and above). In each group, one set of the samples was randomly designated as calibration set (60% of samples) for model development and the remaining as prediction set for validation. Calibration models were compared using the statistics SEC (standard error of calibration), SEP (standard error of prediction corrected for bias), R_C and R_P (correlation coefficients for calibration and prediction, respectively), and bias based on the following formulas:

$$\mathrm{SEC} = \sqrt{\frac{\sum_{i=1}^{N_C} (Y_i - \hat{Y}_i)^2}{N_C - p - 1}} \tag{2}$$

$$\mathrm{SEP} = \sqrt{\frac{\sum_{i=1}^{N_P} (Y_i - \hat{Y}_i - \mathrm{bias})^2}{N_P - 1}} \tag{3}$$

$$\mathrm{bias} = \frac{\sum_{i=1}^{N_P} Y_i}{N_P} - \frac{\sum_{i=1}^{N_P} \hat{Y}_i}{N_P} \tag{4}$$

$$R_C = \frac{N_C \sum_{i=1}^{N_C} Y_i \hat{Y}_i - \left(\sum_{i=1}^{N_C} Y_i\right)\left(\sum_{i=1}^{N_C} \hat{Y}_i\right)}{\sqrt{N_C \sum_{i=1}^{N_C} Y_i^2 - \left(\sum_{i=1}^{N_C} Y_i\right)^2} \cdot \sqrt{N_C \sum_{i=1}^{N_C} \hat{Y}_i^2 - \left(\sum_{i=1}^{N_C} \hat{Y}_i\right)^2}} \tag{5}$$

$$R_P = \frac{N_P \sum_{i=1}^{N_P} Y_i \hat{Y}_i - \left(\sum_{i=1}^{N_P} Y_i\right)\left(\sum_{i=1}^{N_P} \hat{Y}_i\right)}{\sqrt{N_P \sum_{i=1}^{N_P} Y_i^2 - \left(\sum_{i=1}^{N_P} Y_i\right)^2} \cdot \sqrt{N_P \sum_{i=1}^{N_P} \hat{Y}_i^2 - \left(\sum_{i=1}^{N_P} \hat{Y}_i\right)^2}} \quad (6)$$

where , Y_i and $\hat{Y}_i$ are the measured and predicted firmness values, respectively for sample i; p is the number of wavelengths in the model, N_C and N_P are the number of samples in the calibration and prediction sets, respectively.

To further validate the usefulness of results of the stepwise linear regression analysis and understand the sensitivity of the wavelengths in the models, a comprehensive regression search utilizing all possible combinations in the 71-wavelength set taken from one to five wavelengths was also performed. The same evaluation parameters were computed from all the models using the Statistics Toolbox of MATLAB 6.5 (The Mathworks, Inc., Natick, MA, USA).

RESULTS AND DISCUSSION

1. Profile of samples

Table 1 shows that dimensional profile of both calibration set and prediction set samples were not significantly different. Thus, this ensures that the two sets basically represent the same statistical population of fruits and so that adequate validation of models can be reliably made.

Figure 3 shows a plot of the firmness values at three ripeness maturity levels of strawberries for the entire sample sets. Notice that there was a markedly high variability of firmness values for the 50–60% ripe stage and least with the full-ripe stage. As the strawberry fruits mature, aside from increasingly becoming soft, the firmness approaches to a relatively uniform common value.

2. NIR spectral profile of strawberry

The NIR spectral profile of strawberry is shown in Fig. 4. The spectra are marked with a strong absorption, and hence high data variability, in around 675 nm caused by chlorophyll pigmentation (Chen et al., 2002; McGlone et al., 2002) and at around 980 nm by water. Large difference of reflectance can be observed at 675 nm between the various levels of ripeness maturity, however little difference exists at above 740 nm. The increasing ripeness of fruits corresponds to decreasing chlorophyll content due to the reduction in quantity of the pigment thus the absorbance of light seemed to decrease at 675 nm. The spectral variation in the 800 to 1000 nm range is well

Table 1 Dimensional profile of calibration and prediction set samples.

	Length[ns] mm	Width[ns] mm	Breadth[ns] mm	Mass[ns] gm	Firmness[ns] MPa
Calibration Set					
Mean	48.33	32.41	30.83	18.43	1.72
SD[z]	3.40	2.53	2.24	2.77	0.59
CV[y]	7.0	7.8	7.3	15.0	34.4
Maximum	57.8	39.2	36.7	25.6	3.4
Minimum	39.6	26.5	25.0	13.3	0.8
Prediction Set					
Mean	47.93	33.00	31.18	18.74	1.70
SD	3.24	2.47	2.30	3.08	0.58
CV	6.8	7.5	7.4	16.4	34.4
Maximum	55.4	38.3	35.2	26.3	4.1
Minimum	41.0	28.3	24.2	12.7	0.8

[z] Standard deviation.
[y] Coefficient of variation, %.
[ns] Not significantly different by Student's *t*-test.

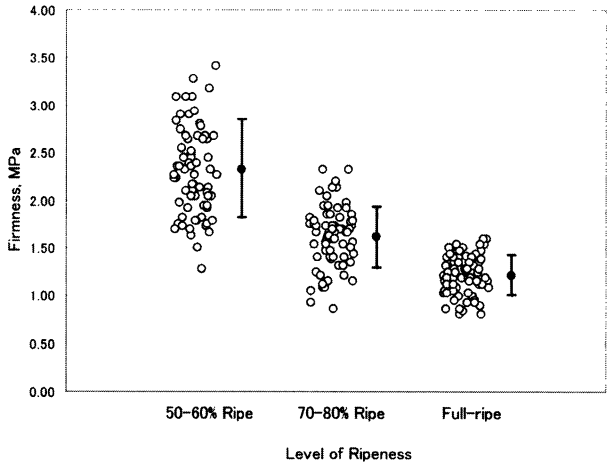

Fig. 3 Profile of firmness at three ripeness maturity levels of strawberry.

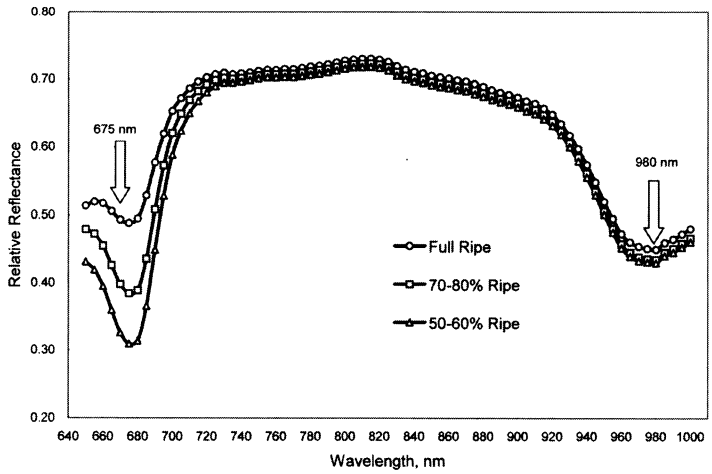

Fig. 4 Diffuse relative reflectance profile with respect to a white reference tile from 650 to 1000 nm spectral images of strawberries at △ 50-60% ripe, □ 70-80% ripe and ○ full-ripe maturity levels.

known for carbohydrates, sugar and water (McGlone et al., 2002). Thus important wavelengths were expected to come from this range to account for the variation of firmness of strawberries. Figure 5 shows some spectral images of samples at three of ripeness maturity levels.

Fruit firmness was found negatively correlated with reflectance values in the entire spectral range, and Fig. 6 shows the absolute value of linear correlation profile. Consistent with the observation with spectral profile, higher correlations were found with the chlorophyll absorption band (660-690 nm) and with the water absorption band around 980 nm.

3. Model development

The characteristics of one- to three-wavelength calibration models for firmness for the two groups of strawberries (70% to full-ripe and 50% to full-ripe) as analyzed by stepwise multiple linear regression are shown in Table 2. To better visualize the fit of the three-wavelength models for the two groups, prediction plots are shown in Fig. 7. The chlorophyll absorption peak close to 680-685 nm (Chen et al., 2002; McGlone et al., 2002) and water at 985-990 nm were significantly

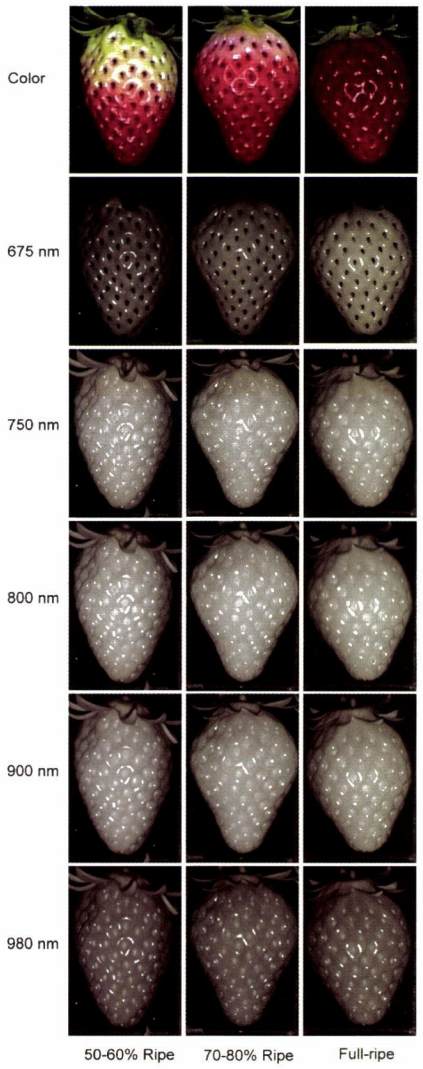

Fig. 5 Images of strawberry samples at 50–60% ripe, 70–80% ripe and full-ripe maturity levels in color and in monochrome at 675, 750, 800, 900, and 980 nm.

included in the models. The general similarity of SEC and SEP values suggests the goodness of fit of the model. However, there seemed to be a better fit of model (higher correlation) when a wider range of samples was considered (50% to full-ripe compared to 70% to full-ripe ranges). This is consistent to the results of the earlier visible range study that dealt with the visible range from which this research had continued. The 680–685 nm wavelength alone accounted for a greater share of variation in firmness that again accentuated the importance of chlorophyll content as an indicator of degree of ripeness maturity, and hence the firmness of strawberries. Although the focal point of this work was in the NIR range, the results had strongly confirmed the importance of a portion of the visible range for firmness prediction. The 985–990 nm range suggested a minor but still important role of water as determinant of the turgidity of the cells that has a relationship to the firmness of fruits. The derived regression equation for the entire range of samples was:

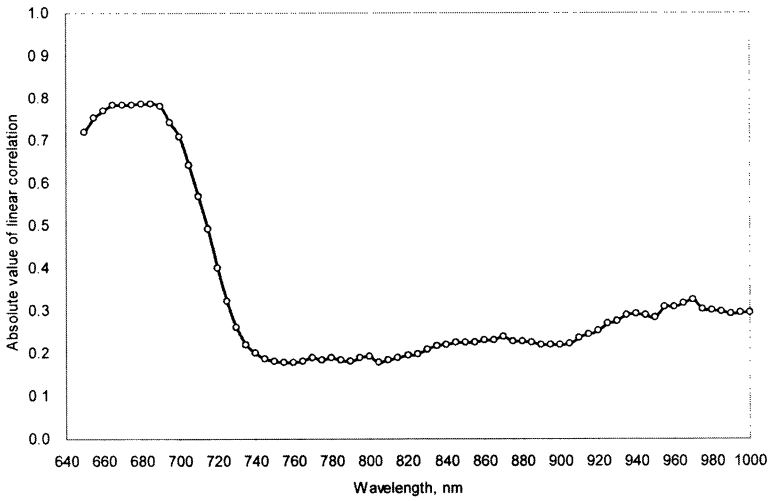

Fig. 6 Plot of absolute value of linear correlation between fruit firmness of strawberries and mean relative diffuse reflectance values from 650 to 1000 nm spectral images.

Table 2 Characteristics of prediction models having different number of wavelengths for estimation of firmness.

Predictors, nm		SEC[z]	R_C[y]	SEP[x]	R_P[w]	Bias
70% to Full-ripe maturity level fruits group						
1	680	0.252	0.702	0.241	0.645	0.025
2	680, 990	0.235	0.750	0.262	0.588	0.041
3	680, 990, 650	0.233	0.760	0.258	0.599	0.033
50% to Full-ripe maturity level fruits group						
1	685	0.356	0.783	0.344	0.796	0.046
2	685, 985	0.342	0.803	0.344	0.794	0.057
3	685, 985, 865	0.338	0.809	0.350	0.786	0.050

[z] Standard error of calibration, MPa.
[y] Correlation coefficient of calibration.
[x] Standard error of prediction, MPa.
[w] Correlation coefficient of prediction.

$$Yp = -6.786\ R_{685} - 6.165\ R_{865} + 13.810\ R_{985} + 2.750 \quad (7)$$

where Yp is the predicted firmness value, and R_{685}, R_{865} and R_{985} are the reflectance values at 685, 865 and 985 nm, respectively.

Figure 8 shows the correlation map between reflectance values at each wavelength. Because of small bandwidth (10 nm) of the filter and fine imaging interval (5 nm), there was a high correlation especially between close or contiguous wavebands. To illustrate, reflectance values at 720 to 910 nm may be used as equivalent estimates for reflectance values for 820 nm (having high correlation at 0.95). This high multi-collinearity of data would suggest that the results of classical stepwise linear regression technique require additional validation to identify significant wavebands. In addition to pinpointing specific center wavelengths, a range of values can be identified for the models. Certainly, this would make the selection of waveband filters easier during technical system design by knowing which wavelength values may be substituted for another.

The comprehensive regression search was done for the entire sample set. The analysis showed

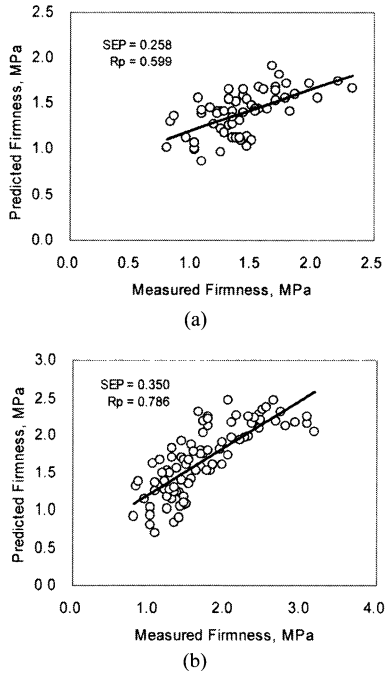

Fig. 7 Prediction plots of the three-wavelength models for estimation of firmness in (a) 70% to full-ripe and (b) 50% to full-ripe strawberries groups.

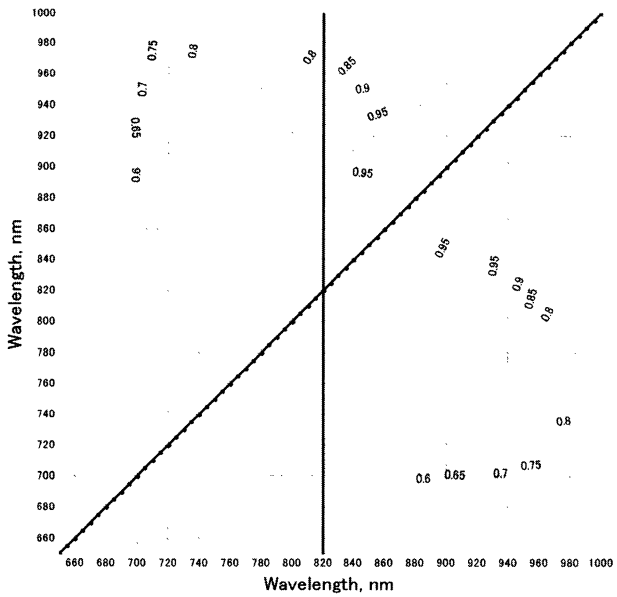

Fig. 8 Correlation map between the reflectance values at each wavelength.

that the same set of wavelengths (685, 865, and 985 nm) had the highest correlation coefficient for calibration for a three-wavelength model. However, some wider ranges of wavebands may be

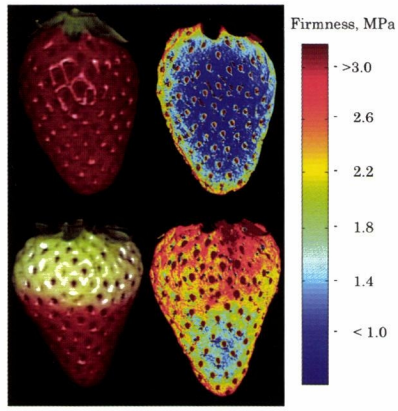

Fig. 9 Pseudo-color maps of firmness distribution in strawberries.

possible having a similar level of performance, and they are listed as follows: 665–685 nm, 755–870 nm, and 955–1000 nm. This means that instead of choosing 685 nm for the first waveband, any filter from 665 to 685 nm would give similar performance.

Using spectral imaging, image maps can be generated using equation 7 to show the distribution of firmness throughout the fruit body. Figure 9 shows some examples of pseudo-color maps that interestingly identify hard and soft regions on the fruits.

In conclusion, hyperspectral imaging in the NIR range has been found useful for non-destructive estimation of internal properties of fruits. Statistical analyses had shown that the three-wavelength model (685, 865, and 985 nm) could predict firmness in strawberries. The more thorough regression analysis found that three ranges of wavebands 670–685 nm, 755–870 nm, and 955–1000 nm could be used to estimate fruit firmness having a similar level of accuracy.

This research was carried out in part through the Grant-In-Aid for Scientific Research (B)(2) No. 15380175, Ministry of Education, Culture, Sports, Science, and Technology. We also wish to acknowledge Mr. Mochihara of Kibana for providing the strawberry samples.

REFERENCES

Abbott, J. A. 1999. Quality measurement of fruits and vegetables. Postharvest Biol. Technol. **15**: 207–225.

Chen, Y., Chao, K., Kim, M. S. 2002. Machine vision technology for agricultural applications. Comput. Electron. Agric. **36**: 173–191.

Cogdill, R. P., Hurburgh, C. R. Jr., Rippke, G. R. 2004. Single-kernel maize analysis by near-infrared hyperspectral imaging. Trans. ASAE **47**: 311–320.

De Ketelaere, B., De Baerdemaeker, J. 2001. Advances in spectral analysis of vibrations for non-destructive determination of tomato firmness. J. Agric. Eng. Res. **78**: 177–185.

Evans, M. D., Thai, C. N., Grant, J. C. 1998. Development of a spectral imaging system based on a liquid crystal tunable filter. Trans. ASAE **41**: 1845–1852.

Ito, H. 2002. Potential of near infrared spectroscopy for nondestructive estimation of Brix in strawberries. Acta Hortic. **567**: 751–754.

Kim, M. S., Chen, Y. R., Mehl, P. M. 2001. Hyperspectral reflectance and fluorescence imaging system for food quality and safety. Trans. ASAE **44**: 721–729.

Kim, M. S., Lefcourt, A. M., Chao, K., Chen, Y. R., Kim, I., Chan, D. E. 2002. Multispectral detection of fecal contamination on apples based on hyperspectral imagery: Part I. Application of visible and near-

infrared reflectance imaging. Trans. ASAE **45**: 2027-2037.

Lammertyn, J., Nicolai, B., Ooms, K., De Smedt, V., De Baerdemaeker, J. 1998. Non-destructive measurement of acidity, soluble solids, and firmness of Jonagold apples using NIR-spectroscopy. Trans. ASAE **41**: 1089-1094.

Lu, R., Ariana, D. 2002. A near-infrared sensing technique for measuring internal quality of apple fruit. Applied Eng. Agric. **18**: 585-590.

Lu, R. 2003. Detection of bruises on apples using near-infrared hyperspectral imaging. Trans. ASAE **46**: 523-530.

Martinsen, P., Schaare, P. N. 1998. Measuring soluble solids distribution in kiwifruit using near-infrared imaging spectroscopy. Postharvest Biol. Technol. **14**: 271-281.

McGlone, V. A., Kawano, S. 1998. Firmness, dry-matter and soluble-solids assessment of postharvest kiwifruit by NIR spectroscopy. Postharvest Biol. Technol. **13**: 131-141.

McGlone, V. A., Jordan R. B., Martinsen, P. J. 2002. Vis/NIR estimation at harvest of pre- and post-storage quality indices for 'Royal Gala' apple. Postharvest Biol. Technol. **25**: 135-144.

Nagata, M., Shrestha, B. P., Gejima, Y. 2001. Study on image processing for quality estimation of strawberries (Part 2): Detection of bruises on fruit by NIR image processing. J. SHITA **14**: 1-9.

Nagata, M., Tallada, J. G., Kobayashi, T., Cui, Y., Gejima, Y. 2004. Predicting maturity quality parameters of strawberries using hyperspectral imaging. ASAE Paper No. 043033. ASAE, St. Joseph, Michigan.

Nagata, M., Tallada, J. G., Kobayashi, T. 2006. Bruise detection using NIR hyperspectral imaging for strawberry (*Fragaria×ananassa Duch.*). Environ. Control Biol. **44**: 133-142.

Peiris, K. H. S., Dull, G. G., Leffler, R. G., Kays, S. J. 1999. Spatial variability of soluble solids or dry-matter content within individual fruits, bulbs, or tubers: Implications for the development and use of NIR spectrometric techniques. HortScience **34**: 114-118.

Saranwong, S., Sornsrivichai, J., Kawano, S. 2004. Prediction of ripe-stage eating quality of mango fruit from its harvest quality measured nondestructively by near infrared spectroscopy. Postharvest Biol. Technol. **31**: 137-145.

Schaare, P. N., Fraser, D. G. 2000. Comparison of reflectance, interactance and transmission modes of visible-near infrared spectroscopy for measuring internal properties of kiwifruit (*Actinidia chinesis*). Postharvest Biol. Technol. **20**: 175-184.

Schmilovitch, Z., Mizrach, A., Hoffman, A., Egozi, H., Fuchs, Y. 2000. Determination of mango physiological indices by near-infrared spectrometry. Postharvest Biol. Technol. **19**: 245-252.

Shewfelt, R. L., Prussia, S. E. ed. 1993. "Postharvest Handling: A Systems Approach". Academic Press, San Diego, pp 358.